Title
Global rates of water-column denitrification derived from nitrogen gas measurements

Journal
Nature Geoscience, 5(8)

ISSN
1752-0894

Authors
DeVries, Tim
Deutsch, Curtis
Primeau, François
et al.

Publication Date
2012-08-01

DOI
10.1038/ngeo1515

nature geoscience

LETTERS

PUBLISHED ONLINE: 8 JULY 2012 | DOI: 10.1038/NGEO1515

Global rates of water-column denitrification derived from nitrogen gas measurements

Tim DeVries[1]*, Curtis Deutsch[1], François Primeau[2], Bonnie Chang[3] and Allan Devol[4]

Biologically available nitrogen (N) limits phytoplankton growth over much of the ocean. The rate at which N is removed from the contemporary ocean by denitrifying bacteria is highly uncertain[1–3]. Some studies suggest that N losses exceed inputs[2,4–6]; others argue for a balanced budget[3,7,8]. Here, we use a global ocean circulation model to simulate the distribution of N_2 gas produced by denitrifying bacteria in the three main suboxic zones in the open ocean. By fitting the model to measured N_2 gas concentrations, we infer a globally integrated rate of water-column denitrification of 66 ± 6 Tg N yr^{-1}. Taking into account isotopic constraints on the fraction of denitrification occurring in the water column versus marine sediments, we estimate that the global rate of N loss from marine sediments and the oceanic water column combined amounts to around 230 ± 60 Tg N yr^{-1}. Given present estimates of N input rates, our findings imply a net loss of around 20 ± 70 Tg of N from the global ocean each year, indistinguishable from a balanced budget. A balanced N budget, in turn, implies that the marine N cycle is governed by strong regulatory feedbacks.

The loss of N in the ocean occurs as bacteria reduce N to N_2 gas through a combination of heterotrophic denitrification and anaerobic ammonium oxidation (hereafter collectively termed denitrification). Suboxic conditions in which O_2 is scarce enough to favour these processes are found in three principal locations in the water column: the Arabian Sea, the eastern tropical South Pacific (ETSP) and the eastern tropical North Pacific (ETNP; Fig. 1). Denitrification rates in these areas estimated from nitrate deficits and water-mass age tracers yield a global rate of water-column denitrification in the range of 60–90 Tg N yr^{-1} (refs 9–14), but recently rates as large as 150 Tg N yr^{-1} have been proposed[2]. Denitrification also occurs in suboxic pore waters of sediments throughout the ocean, but the rates are spatially heterogeneous and have been measured at only a handful of sites[15], precluding a direct global estimate. However, the global rate of sedimentary N loss (primarily denitrification, but also a small burial of organic N) is constrained by the isotopic ratio of mean ocean nitrate to be one to four times as large as the rate of denitrification in the suboxic water column[6,16,17]. Estimates of the total rate of N loss in the ocean therefore inherit and amplify the uncertainty in the rate of denitrification in suboxic waters, yielding a combined rate of about 270 Tg N yr^{-1} (ref. 3) to more than 400 Tg N yr^{-1} (refs 2,6). These rates far exceed the estimated global rate of N fixation, which is in the range of 100–160 Tg N yr^{-1} (refs 7,18). The apparent deficit is partially offset by riverine and atmospheric inputs of about 40–125 Tg N yr^{-1} (refs 3,15). Still, if the upper end of the denitrification-rate estimates are correct, the ocean must be rapidly losing fixed N.

The wide range of estimates of water-column denitrification rate[9–14] reflects uncertainties in nutrient stoichiometries and the volume of suboxic waters, and is further exacerbated by the limits of simple mixing models and transient age tracers, especially in poorly ventilated waters[14]. To reduce these uncertainties requires robust tracers of net N loss and the ability to accurately account for the physical transport in and around suboxic zones. Recent advances in numerical modelling allow equilibrium tracer distributions to be rapidly computed from arbitrary sources and sinks embedded in a global three-dimensional circulation constrained by observations[19]. Meanwhile, the concentrations of N_2 gas have recently been measured with sufficient precision and accuracy in all three suboxic zones to determine the excess of N_2 relative to background levels. This excess N_2 (N_{xs}) provides a direct measure of the net loss of N that is independent of the metabolic pathway (Fig. 1; see refs 20,21; B. X. Chang, A. H. Devol and S. R. Emerson, manuscript in preparation).

Using a data-constrained ocean circulation model, we computed the global rates of water-column denitrification needed to match the observed N_{xs} in all three suboxic zones. The circulation model has been optimized to closely reproduce observed temperature, salinity, radiocarbon and CFC-11 concentrations using an adjoint method (see Supplementary Methods and ref. 19), so that the transport and mixing of N_{xs} is maximally consistent with both the large-scale momentum balance and all relevant tracer observations. A good measure of the fidelity of the model ventilation in suboxic zones is its predicted CFC-11 concentrations, which deviate from observations by less than 5% in the three main suboxic zones (Supplementary Figs S1 and S2).

The simulated production of N_{xs} is confined to observed suboxic zones and is distributed within them in proportion to satellite-based estimates of organic-matter production and parameterized vertical profiles of sinking particulate flux (see Supplementary Methods). To account for uncertainty in the true volume of denitrifying waters, we vary the critical O_2 threshold used to bound the denitrifying water mass. We also sample a range of coefficients for the vertical attenuation of the organic-matter flux, to account for uncertainty in the vertical gradient of the denitrification rate. To reflect uncertainty in the carbon export flux and the stoichiometry of organic matter, we vary the ratio of the number of moles N consumed during microbial respiration of one mole organic carbon under suboxic conditions. These parameters are varied so as to fit the model to the N_{xs} observations using a Markov–Chain Monte Carlo (MCMC) approach (see Supplementary Methods and Fig. S3). The MCMC simulation propagates uncertainty in model parameters to uncertainty in the model-estimated N-loss rates in each suboxic zone, providing a rigorous error estimate characterized by the

[1]Department of Atmospheric and Oceanic Sciences, University of California, Los Angeles, California 90095, USA, [2]Department of Earth System Science, University of California, Irvine, California 92697, USA, [3]Department of Geosciences, Princeton University, Princeton, New Jersey 08544, USA, [4]School of Oceanography, University of Washington, Seattle, Washington 98195, USA. *e-mail: tdevries@atmos.ucla.edu.

NATURE GEOSCIENCE DOI: 10.1038/NGEO1515

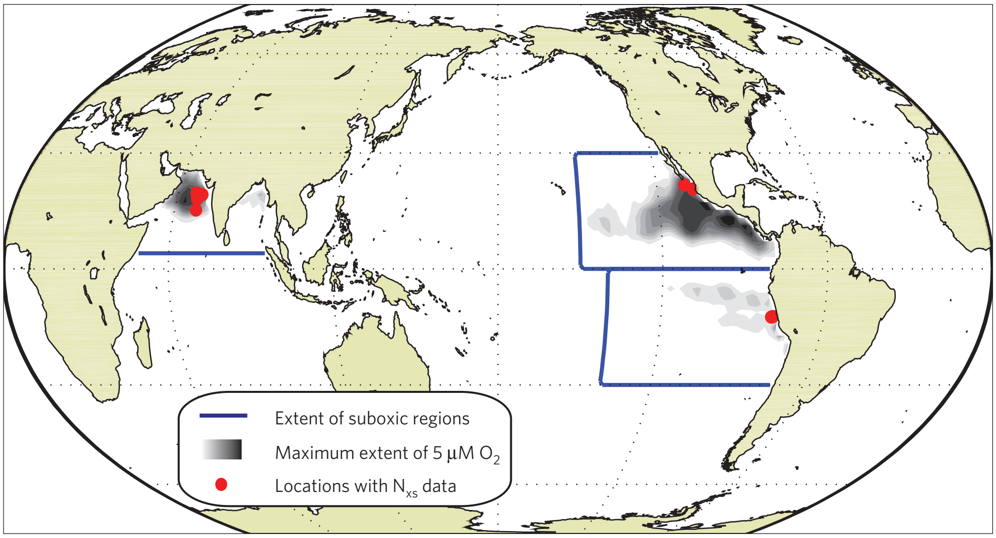

Figure 1 | Suboxic zones and data locations. Map showing the location of the three main suboxic zones in the Arabian Sea, the ETSP and the ETNP. Solid blue lines mark the regions in which water-column denitrification is allowed to occur in the model. Grey shading represents the frequency with which the observed O_2 concentration falls below 5 μM. Circles mark locations with N_{xs} observations. N_{xs}, excess N_2.

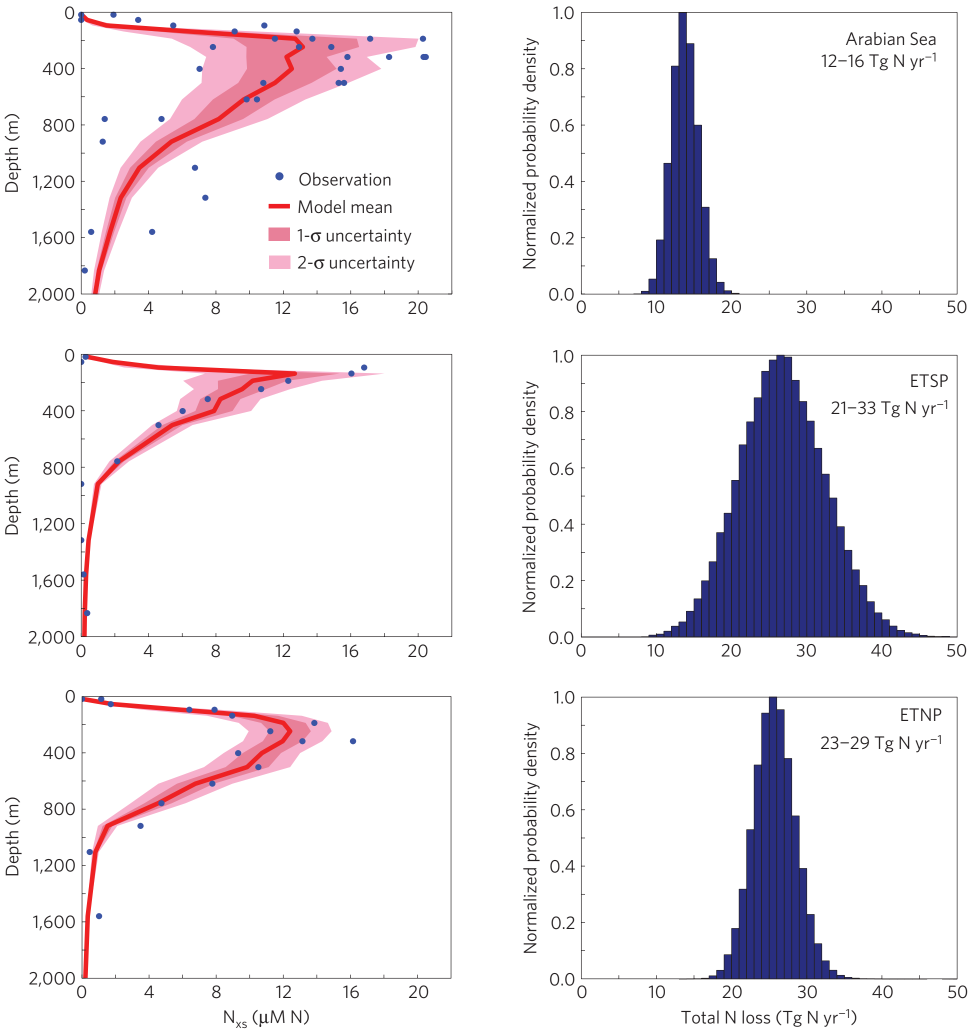

Figure 2 | Modelled N_{xs} and total N loss. Results of the MCMC simulations showing model fit to the data in each suboxic zone and the posterior p.d.f. of total N loss in each region. The range of total N loss given next to each p.d.f. is the 1-σ confidence interval. The solid line in each plot on the left-hand side is the mean modelled N_{xs} concentration at each depth, averaged over all locations where there are data and over all model runs. p.d.f., probability density function; N_{xs}, excess N_2.

probability density function (p.d.f.) for integrated denitrification rates in each region (Fig. 2).

Using this method we infer that the global rate of water-column denitrification is 66 ± 6 Tg N yr^{-1}. The Arabian Sea, for which the most data are available, shows both the lowest denitrification rates and the smallest uncertainty (12–16 Tg N yr^{-1} at a 1-σ confidence level). Previous estimates of water-column denitrification in the Arabian Sea calculated a total N loss of 13–41 Tg N yr^{-1} (for example, ref. 20). In the ETSP, our simulations suggest that the rate of water-column denitrification is 21–33 Tg N yr^{-1}, whereas that in the ETNP is 23–29 Tg N yr^{-1} (Fig. 2). The combined rate of denitrification in the eastern tropical Pacific is 46–58 Tg N yr^{-1}, which is close to a previously estimated rate of 43–53 Tg N yr^{-1} based on nitrate deficit calculations[14]. The rate calculated for the eastern tropical Pacific is more uncertain than that for the Arabian Sea primarily because of the sparser data coverage.

The rates estimated here represent an average over a time period similar to the residence time of waters in the suboxic zones. In the Pacific, denitrification rates inferred from nutrient measurements off southern California and from hindcast model simulations seem to be highly variable over decadal timescales, with relatively high rates in the most recent decade when the N_2 measurements were made[22]. Thus the long-term rates of denitrification in the Pacific may be lower than calculated here.

The integrated N-loss rates derived here are robust and insensitive to large variations in the model parameters. Despite large uncertainties (~50%) in the values of the model parameters (see Supplementary Discussion and Table S1), the uncertainty in the globally integrated N-loss rate is low (~10%) and is mostly uncorrelated with those parameters (Supplementary Fig. S4). This indicates that any potential biases in the inferred values of the uncertain parameters have little effect on the integrated N-loss rates. It is particularly important that the total N-loss rate is insensitive to the critical O_2 threshold and therefore to the total volume of the denitrifying water mass (Supplementary Fig. S4). This is because to match the observed N_{xs} concentrations, the model maintains an inverse relationship between the volume of the putative denitrifying water mass and the volumetric denitrification rate within it. That is, if we assume a larger suboxic volume, the model will choose a smaller rate of denitrification to match the observed N_{xs} concentrations. In contrast, denitrification rates predicted by geochemical methods depend strongly on the poorly known O_2 threshold and the associated suboxic volume.

The formal error estimate of 10% takes into account uncertainty in the observations and in the model parameters. Additional sources of uncertainty that are more difficult to quantify include that associated with the circulation model and with the parameterization of organic-matter export fluxes. To explore these sources of uncertainty we carried out sensitivity experiments in which we varied transport rates and the parameterization of organic-matter fluxes in the suboxic zones (Supplementary Fig. S5 and Table S2). These experiments constitute a very strict test of the robustness of the results and demonstrate that the uncertainty in the integrated N-loss rates derived here is almost certainly not greater than 20%.

The rate of denitrification calculated here is lower than some previous estimates that were based on geochemical methods[9–14]. The difference cannot be attributed to any single factor and a detailed comparison of the various methods of determining denitrification rates is beyond the scope of this study. However, simple geochemical methods applied to model tracer fields are generally unable to accurately reconstruct the associated N-loss rates, owing to several sources of bias (Supplementary Fig. S6 and Table S3). The spatially explicit model used here accounts for spatial variability in denitrification rates, ocean circulation and mixing processes within the suboxic zones,

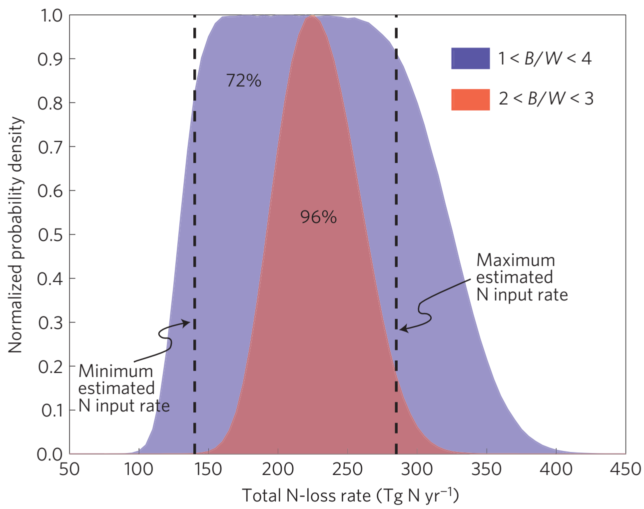

Figure 3 | Marine N budget. Total marine N-loss rates based on our estimated rate of water-column denitrification (66 ± 6 Tg N yr^{-1}) and isotopic constraints on the ratio of B to W. Blue shading is the p.d.f. of N losses assuming $1 < B/W < 4$ with uniform probability; red shading denotes the more conservative range of $2 < B/W < 3$. Estimated rates of total N inputs (including N fixation, atmospheric and riverine inputs) are taken from the literature[3,7,15,18]. Numbers printed on each p.d.f. represent the proportion of the p.d.f. that falls within the maximum and minimum estimated N input rates. B, rate of benthic N removal; W, rate of water-column denitrification.

and thus provides a more accurate rate estimate than typical geochemical methods.

Rates of water-column denitrification have important implications for the global marine N budget. The global marine N budget imbalance, ΔN, can be written

$$\Delta N = I - W - B \quad (1)$$

where I is the total rate of oceanic N input, W is the rate of water-column denitrification and B is the rate of benthic N removal (sedimentary denitrification plus a small burial of organic N). The isotopic ratio of mean ocean nitrate constrains the ratio of benthic to water-column denitrification to be in the range of $1 < B/W < 4$ (refs 6,16,17). Given these constraints and the estimate of W derived here, we estimate that the total rate of oceanic N loss is about 230 ± 60 Tg N yr^{-1}. The p.d.f. for total N loss is shown in Fig. 3 (blue shading). The bulk (72%) of the p.d.f. for total N loss occurs within present estimates of the total rate of N input, which range from 140 Tg N yr^{-1} to 285 Tg N yr^{-1}. Only 23% of the p.d.f. for total N loss lies beyond 285 Tg N yr^{-1}, whereas 5% lies below 140 Tg N yr^{-1}. The net N budget imbalance, calculated from equation (1) and assuming the p.d.f. for N inputs is uniform between 140 and 285 Tg N yr^{-1}, is $\Delta N = -19 \pm 74$ Tg N yr^{-1}, implying that any imbalance in the N budget is virtually indistinguishable from zero. Using a more conservative range of $2 < B/W < 3$, based on results from a multibox model[16], 96% of the p.d.f. for total N losses falls within the estimated range of oceanic N inputs (Fig. 3, red shading), leaving very little room for imbalance in the oceanic N budget.

This study is an important step towards constraining the total rate of N loss in the ocean. The denitrification rates inferred here offer little support for an imbalance in the oceanic N budget. However, important uncertainties remain in other terms in the N budget and these will have to be better constrained before one can say definitively if the oceanic N budget is balanced. Given the sparsity of direct measurements of the rates of these processes, inverse models that combine geochemical tracer data with models of ocean circulation to infer globally integrated rates seem to hold great potential for resolving persistent uncertainties in the marine N cycle.

Methods

Data-constrained ocean circulation model. The circulation model is based on the data-constrained model of ref. 19 and is fit to climatological potential temperature, salinity and natural radiocarbon distributions, as well as climatological mean sea surface height, sea surface heat fluxes and sea surface freshwater fluxes. Here we have extended this work by increasing the model resolution to two degrees in the horizontal and by using CFC-11 bottle data from the Global Ocean Data Analysis Project[23] to further constrain the circulation model. CFC-11 is modelled following the Ocean–Carbon Cycle Model Intercomparison Project Phase 2 protocols[24]. The model achieves a good fit to the CFC-11 data, with a globally averaged root mean squared model data misfit of 0.20 $pmol\,kg^{-1}$.

N_{xs} simulations. N_{xs} is modelled with a source in the water column where the observed O_2 concentration[25] falls below a critical threshold $O_{2,crit}$ and an effective sink owing to gas exchange with a well-mixed atmosphere at a piston velocity of 3 $m\,d^{-1}$. The production of N_{xs} is assumed to be proportional to the remineralization of organic carbon, which is parameterized with a power-law dependence on depth using export production rates derived from satellite-based estimates of net primary production[26,27] and an empirically determined export ratio[28]. See Supplementary Methods for further details.

MCMC simulations. A posterior p.d.f. was defined to measure the misfit between modelled and observed N_{xs} and to capture an appropriate parameter space defined by previous p.d.fs for the model parameters (see Supplementary Methods and Fig. S3). MCMC simulations were carried out by running 18 chains independently, starting with an initial random draw from an appropriately overdispersed distribution of the model parameters and ending when 5,000 samples had been drawn from the posterior p.d.f. We removed the first 1,000 samples from each chain to ensure that the initial condition had been forgotten and the remaining 72,000 parameter sets ($18 \times 4,000$) were used to calculate the rate of N loss in each suboxic zone, producing the plots in Fig. 2. See Supplementary Methods for further details.

Received 20 January 2012; accepted 6 June 2012; published online 8 July 2012

References

1. Codispoti, L. A. *et al.* The oceanic fixed nitrogen and nitrous oxide budgets: Moving targets as we enter the anthropocene. *Scientia Marina* **65,** 85–105 (2001).
2. Codispoti, L. An oceanic fixed nitrogen sink exceeding 400 $Tg\,N\,a^{-1}$ vs. the concept of homeostasis in the fixed-nitrogen inventory. *Biogeosciences* **4,** 233–253 (2007).
3. Gruber, N. in *Nitrogen in the Marine Environment* (eds Capone, D. G., Bronk, D. A., Mulholland, M. R. & Carpenter, E. J.) 1–50 (Elsevier, 2008).
4. Codispoti, L. Is the ocean losing nitrate? *Nature* **376,** 724 (2002).
5. Middelburg, J., Soetart, K., Herman, P. M. J. & Heip, C. H. R. Denitrification in marine sediments: A model study. *Glob. Biogeochem. Cycles* **10,** 661–673 (1996).
6. Brandes, J. A. & Devol, A. H. A global marine-fixed nitrogen isotopic budget: Implications for holocene nitrogen cycling. *Glob. Biogeochem. Cycles* **16,** 1120 (2002).
7. Gruber, N. & Sarmiento, J. Global patterns of marine nitrogen fixation and denitrification. *Glob. Biogeochem. Cycles* **11,** 235–266 (1997).
8. Gruber, N. in *The Ocean Carbon Cycle and Climate* (eds Follows, M. & Oguz, T.) 97–148 (Kluwer Academic, 2004).
9. Codispoti, L. A. & Richards, F. A. An analysis of the horizontal regime of denitrification in the eastern tropical North Pacific. *Limnol. Oceanogr.* **21,** 379–388 (1976).
10. Naqvi, S. W. A. Some aspects of the oxygen-deficient conditions and denitrification in the Arabian Sea. *J. Mar. Res.* **45,** 1049–1072 (1987).
11. Fauzi, R. *et al.* Nitrogen biogeochemical cycling in the northwestern indian ocean. *Deep Sea Res.* **40,** 651–671 (1993).
12. Howell, E. A., Doney, S. C., Fine, R. A. & Olson, D. B. Geochemical estimates of denitrification in the Arabian Sea and Bay of Bengal during WOCE. *Geophys. Res. Lett.* **24,** 2549–2552 (1997).
13. Bange, H. W. *et al.* A revised nitrogen budget for the Arabian Sea. *Glob. Biogeochem. Cycles* **14,** 1283–1297 (2000).
14. Deutsch, C., Gruber, N., Key, R. M., Sarmiento, J. L. & Ganachaud, A. Denitrification and N_2 fixation in the Pacific Ocean. *Glob. Biogeochem. Cycles* **15,** 483–506 (2001).
15. Galloway, J. N. *et al.* Nitrogen cycles: Past, present, and future. *Biogeochemistry* **70,** 153–226 (2004).
16. Deutsch, C., Sigman, D. M., Thunell, R. C., Meckler, A. N. & Haug, G. H. Isotopic constraints on glacial–interglacial changes in the oceanic nitrogen budget. *Glob. Biogeochem. Cycles* **18,** GB4012 (2004).
17. Altabet, M. A. Constraints on oceanic N balance/imbalance from sedimentary ^{15}N records. *Biogeosciences* **4,** 75–86 (2007).
18. Deutsch, C., Sarmiento, J. L., Sigman, D. M., Gruber, N. & Dunne, J. P. Spatial coupling of nitrogen inputs and losses in the global ocean. *Nature* **445,** 163–167 (2007).
19. DeVries, T. & Primeau, F. Dynamically- and observationally-constrained estimates of water-mass distributions and ages in the global ocean. *J. Phys. Ocean.* **41,** 2381–2401 (2011).
20. Devol, A. H. *et al.* Denitrification rates and excess nitrogen gas concentrations in the Arabian Sea oxygen deficient zone. *Deep Sea Res. I* **53,** 1533–1547 (2006).
21. Chang, B. X., Devol, A. H. & Emerson, S. R. Denitrification and the nitrogen gas excess in the eastern tropical South Pacific oxygen deficient zone. *Deep Sea Res. I* **57,** 1092–1101 (2010).
22. Deutsch, C., Brix, H., Ito, T., Frenzel, H. & Thompson, L. Climate-forced variability of ocean hypoxia. *Science* **333,** 336–339 (2011).
23. Key, R. M. *et al.* A global ocean carbon climatology: Results from GLODAP. *Glob. Biogeochem. Cycles* **18,** GB4031 (2004).
24. Najjar, R. & Orr, J. Design of OCMIP-2 simulations of chlorofluorocarbons, the solubility pump and common biogeochemistry. http://www.ipsl/jusiieu.fr/OCMIP/phase2/#simulations (1998).
25. Garcia, H. E. *et al.* in *World Ocean Atlas 2009* (ed. Levitus, S.) (US Government Printing Office, 2010).
26. Behrenfeld, M. J. & Falkowski, P. G. Photosynthetic rates derived from satellite-based chlorophyll concentration. *Limn. Ocean.* **42,** 1–20 (1997).
27. Westberry, T., Behrenfeld, M. J., Siegel, D. A. & Boss, E. Carbon-based primary production modeling with vertically resolved photoacclimation. *Glob. Biogeochem. Cycles* **22,** GB2024 (2008).
28. Dunne, J. P., Armstrong, R. A., Gnanadesikan, A. & Sarmiento, J. L. Empirical and mechanistic models for the particle export ratio. *Glob. Biogeochem. Cycles* **19,** GB4026 (2005).

Acknowledgements

This study was supported by NSF grants OCE-1131548 and OCE-1131768 and by the Gordon and Betty Moore Foundation.

Author contributions

C.D. and T.D. designed the study. T.D. carried out the simulations. T.D. and C.D. wrote the paper, with input from B.C., A.D. and F.P. T.D. and F.P. designed the ocean circulation model. B.C. and A.D. provided the N_{xs} data.

Additional information

The authors declare no competing financial interests. Supplementary information accompanies this paper on www.nature.com/naturegeoscience. Reprints and permissions information is available online at www.nature.com/reprints. Correspondence and requests for materials should be addressed to T.D.